SLAC-PUB-10164
September 2003

Build up of Electron Cloud in the PEP-II Particle Accelerator in the Presence of a Solenoid Field and with Different Bunch Pattern*

Y. Cai and M. Pivi
Stanford Linear Accelerator Center
Stanford University
Menlo Park, CA 94025

M. A. Furman
Center for Beam Physics
Accelerator and Fusion Research Division
Lawrence Berkeley National Laboratory, MS 71-259
Berkeley, CA 94720

Abstract

We have augmented the code POSINST to include solenoid fields, and used it to simulate the build up of electron cloud due in the PEP-II positron ring. We find that the distribution of electrons is strongly affected by the resonances associated with the cyclotron period and bunch spacing. In addition, we discover a threshold beyond which the electron density grows exponentially until it reaches the space charge limit. The threshold does not depend on the bunch spacing but does depend on the positron bunch population.

(Submitted to Physical Review Special Topics: Accelerators and Beams)

*Work supported by the Department of Energy under Contract No. DE-AC03-76SF00515 and DE-AC03-76SF00098.

Build up of Electron Cloud in the PEP-II Particle Accelerator in the Presence of a Solenoid Field and with Different Bunch Pattern

Y. Cai and M. Pivi*
SLAC, Stanford University, 2575 Sand Hill Road, Menlo Park, CA 94025.

M. A. Furman†
Center for Beam Physics
Accelerator and Fusion Research Division
Lawrence Berkeley National Laboratory, MS 71-259
Berkeley, CA 94720
(Dated: **DRAFT:** September 10, 2003)

We have augmented the code POSINST to include solenoid fields, and used it to simulate the build up of electron cloud due in the PEP-II positron ring. We find that the distribution of electrons is strongly affected by the resonances associated with the cyclotron period and bunch spacing. In addition, we discover a threshold beyond which the electron density grows exponentially until it reaches the space charge limit. The threshold does not depend on the bunch spacing but does depend on the positron bunch population.

PACS numbers: 29.27.Bd,79.20.Hx,29.20.Dh
Keywords: Electron-cloud effect.

I. INTRODUCTION

It is well established by many experimental evidences [1, 2] at KEKB and PEP-II that the instabilities caused by electron impose a severe limitation upon the luminosity in e^+e^- storage rings. Based on the experiments [1] at KEKB, there exists a current threshold beyond which the vertical beam size at the interaction point starts to grow like $\sigma_y^* \propto N_p^2/S_b$, where N_p is the bunch population and S_b is the spacing between two sequential bunches. Since N_p is normally set at the limit allowed by the beam-beam interaction, this observation implies that S_b cannot be too small otherwise the vertical blow-up degrades the luminosity. As a result, both B-factories are currently operated $S_b \approx 2$ m, which is larger than its design value.

Experimentally, the solenoid field raises the threshold of the blow-up and therefore allows the increase of luminosity. On the other hand, we know from the simulation performed by Zimmermann [3] that longitudinal solenoid field B_s confines the electrons near the wall of the vacuum chamber and therefore reduces the cloud density near the positron beam. All this indicates that both S_b and B_s play vital roles in the physics of electron cloud instability. In this paper, we will study the dynamics between the positron beam and electron cloud with different S_b and B_s to reveal the physics indicated from the simulations and experiments in the PEP-II low energy ring (LER).

*Electronic address: yunhai@slac.stanford.edu,mpivi@slac.stanford.edu
†Electronic address: mafurman@lbl.gov

II. PHYSICAL MODEL

A. Sources of Electrons

The main sources of electrons in the PEP-II are given by: residual gas ionization, photoemission from synchrotron radiation and secondary emission from electrons hitting the walls. In the present simulations we initially generate a certain large number of electrons uniformly (in azimuth) at the chamber wall and let the electron cloud develops by the secondary emission process until an equilibrium (saturation) density is reached. This approach is valid in the limit that small number of electrons are generated at each bunch passage compared to the equilibrium level.

B. Secondary Emission Process

The secondary electron yield (SEY) $\delta(E_0)$ and the corresponding emitted-electron energy spectrum $d\delta/dE$ (E_0 =incident electron energy, E = emitted secondary energy) are represented by a detailed model described elsewhere [4]. The parameters have been obtained from detailed fits to the measured SEY of various materials [5]. The main SEY parameters are the energy $E_{\max}$ at which $\delta(E_0)$ is maximum and the peak value $\delta_{\max} = \delta(E_{\max})$, see Table I and Fig 1. To be consistent with our previous simulations we have used a value for $\delta_{\max} \sim 2.0$ and $E_{\max}$=300 eV. Furthermore, for the results shown below, we do take into account the elastic backscattered and rediffused components of the secondary emitted-electron energy spectrum $d\delta/dE$ at $E_0 \simeq 0$. The backscattered component typically becomes more important at low incident electron energies. To account for this behavior we have used a fit extrapolated data for copper measured at

CERN [6] and assumed a $\delta(0) \simeq 0.5$ corresponding to a 50% reflectivity for electrons impinging the wall with an energy close to 0 eV.

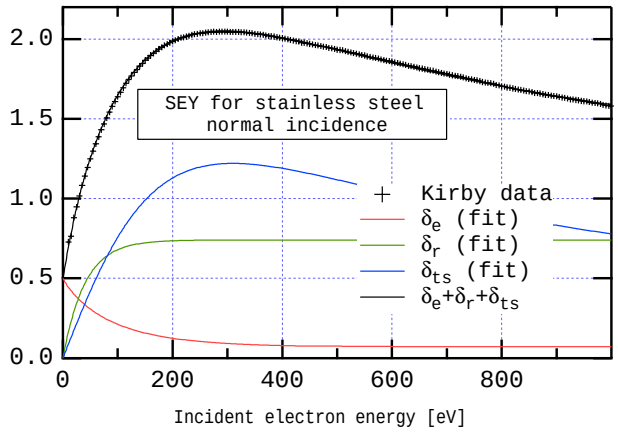

FIG. 1: (Color) The SEY for stainless steel for a SLAC standard 304 rolled sheet, chemically etched and passivated but not conditioned. Shown in figure the fit to the SEY experimental data and the contributions from the three physical effects of the secondary emission process namely the true secondary, elastic backscattered and rediffused components.

C. Simulation Model

For the purpose of these present studies we simulate the passage of a train consisting of PEP-II bunches with a bunch population of 1×10^{11} and having a 4 or 2 bucket spacing, corresponding to 8.4 and 4.2 nsec. The stainless steel vacuum chamber is assumed to be a cylindrical perfectly-conducting round pipe with a 45 mm radius.

Typically, the electrons are simulated by macro-particles, each one representing a defined number of electrons and carrying a fixed charge as described in [7]. The secondary electron emission mechanism adds to these a variable number of macro-particles, generated according to the SEY model mentioned above. The bunch is divided up into N_k slices (51) and the inter-bunch gap into N_g (250) intermediate steps. The image and space charge forces are computed and applied at each slice in the bunch and each step in the gap. Typical beam and vacuum chamber parameters are listed in Table I.

For simplicity, we assume that the bunch travels at the speed of light and since the beam electric field is effectively two-dimensional, it is convenient to use complex notation to represent it [7, 8].

D. Electron Motion

Our work starts with implementing longitudinal solenoid field in the code POSINST [7]. For simplicity, we assume that $\vec{B}$ is a constant and ignore any end effects of the solenoid. For a relativistic electron, the equation of motion can be written

$$\dot{\vec{v}} = -\vec{v} \times \frac{e\vec{B}}{\gamma mc} = \vec{\omega} \times \vec{v} \tag{1}$$

where $\vec{\omega} = e\vec{B}/\gamma mc$ is the cyclotron frequency of the electron. The solution of Eq. (1) is a helical orbit with the axis of the helix parallel to the magnetic field and the Larmor radius $r = v_\perp/\omega$. Along the field, electron moves in a constant speed $v_\parallel$. This solution is programmed in the code to compute the motion of the electrons where the solenoid field is at presence.

TABLE I: Simulation parameters for the PEP-II LER

Parameter	Description	LER
E(Gev)	beam energy	3.1
C(m)	circumference	2200
N_p	bunch population	1.0×10^{11}
$\bar{\beta}$(m)	average beta function	17.0
$\epsilon_{x,y}$(nm-rad)	emittance x,y	24.0, 3.0
σ_z(cm)	bunch length	1.3
S_{RF}(m)	RF bucket spacing	0.63
δ_{max}	max secondary yield	2.0
E_{max}(eV)	energy at yield max	300
$\delta(0)$	yield low energy el.	0.5
r_b(cm)	beam pipe radius	4.5

The parameters used in the simulation is tabulated in Table I. S_b has to be a multiple of the RF spacing S_{RF}. N_p corresponds to the value at the peak of a typical fill in the recent operation.

III. SIMULATION RESULTS

A. Bunch Train

Our simulation focuses on the electrons accumulated through the secondary emission from the beam pipe in the straight sections where not many primary electrons should be generated because of lack of synchrotron radiation.

The bunch pattern used in the simulation consists of a short train, long abort gap, and a long train. The density of electron cloud is clearly building up along the long train after the gap as shown in Fig. 2. Without solenoid field, the average density grows extremely fast along the train but saturates quickly near twice the neutralization density $\rho_e = N_p/\pi r_b^2 S_b$ due to the balance between the space charge and secondary yield. As the solenoid field increases, both the growth rate and the equilibrium level decrease. At $B_s = 15$ G, we see a very gradual growth

of the density along the train of 600 bunches. Assuming that the cloud density is proportional to the vertical beam blow-up, this simulation may be used to explain the observation of the very slow blow-up along the train after the initial installation of the solenoids at KEKB [1]. As B_s reaches 25 G, the average electron density does not grow and is kept below 5% of ρ_e. That is near the density at which the head-tail instability occurs in the LER [9]. Fortunately, the density near the beam drops even more since the solenoid field restraints the electrons near the wall.

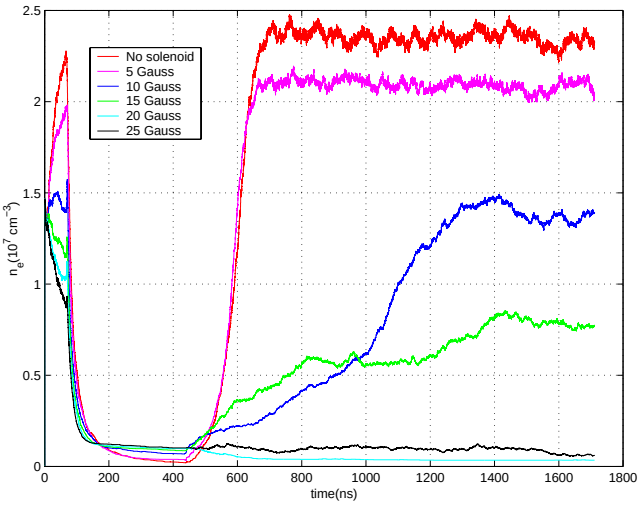

FIG. 2: Density of electron cloud as a function of time when a bunch train passes through a stainless-steel beam pipe and longitudinal solenoid at different settings. The bunch spacing $S_b = 2S_{RF}$.

B. Cyclotron Resonance

As B_s increases further, we find at 40 G that the equilibrium density along the bunch train actually become larger than the density without solenoid as shown in Fig. 3 for a bunch spacing $S_b = 2S_{RF}$ and in Fig. 4 for a bunch spacing $S_b = 3S_{RF}$. However, we observed that most of the electrons are confined in the vicinity of the wall as shown in Fig. 5. It is clearly seen from Figs 3and 4 that this phenomenon appears as a multipacting resonance. Indeed, the result can be explained by a resonance of multipacting associated with the cyclotron frequency ω and the bunch spacing S_b. Given the low-energy nature of the secondary electrons (100 eV), the radius of cyclotron motions is much smaller than the radius of beam pipe. The time of flight of an electron being emitted at the wall, bending back by the magnetic field and finally hitting the wall is nearly half of the cyclotron period $T_c = 2\pi/\omega$. The resonance occurs when the time of flight coincides with the time interval between two consecutive bunches, namely

$$T_c/2 = S_b/c. \tag{2}$$

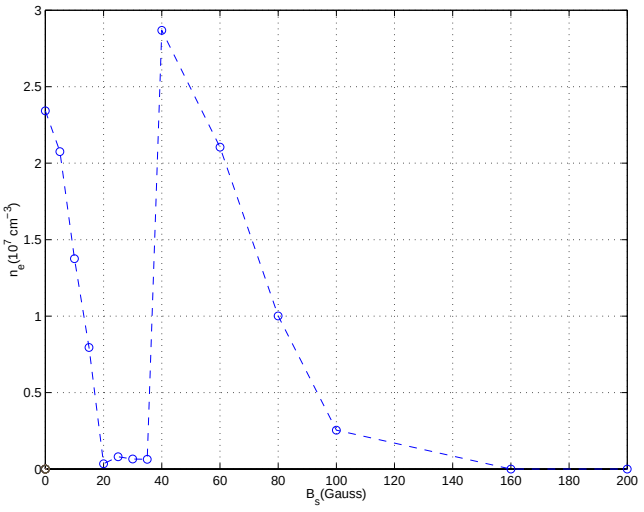

FIG. 3: Equilibrium electron-cloud density along the bunch train as a function of solenoid field. The bunch spacing $S_b = 2S_{RF}$.

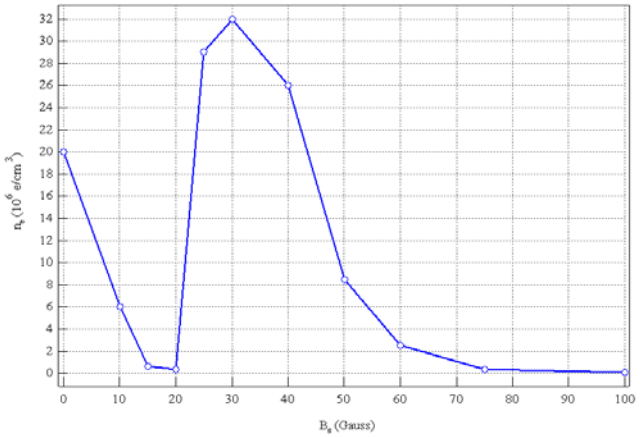

FIG. 4: Equilibrium electron-cloud density along the bunch train as a function of solenoid field. The bunch spacing $S_b = 3S_{RF}$.

Since $\gamma \approx 1$ for typical secondary electrons, this resonance is almost independent of the velocities of electron and therefore much stronger than the resonance occurred in drift space [10]. The condition of cyclotron resonance is given by

$$B_s^c = \frac{\pi mc^2}{eS_b}. \tag{3}$$

Given $S_b = 1.26$ m, we have $B_s^c = 40$ G. That agrees with the simulation. In addition, we can see from Fig. 3 that a minimum density occurs at $B_s = B_s^c/2$. If the bunch spacing is increased to $S_b = 3S_{RF}, 4S_{RF}$, B_s^c is reduced to 30 G, 20 G according to Eq. (3), as shown in Fig. 4 for the case $S_b = 3S_{RF}$. Indeed, that is well confirmed by simulations and by a different approach using Vlasov equation in [11]. Moreover, we find that the characters of dynamics are essentially the same if we keep the product

of S_b and B_s as a constant.

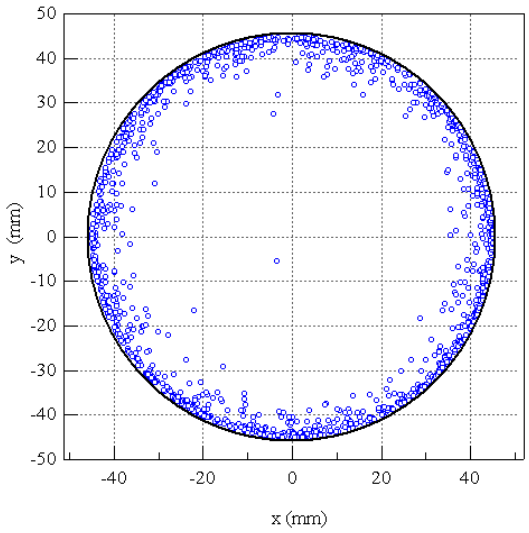

FIG. 5: Snapshot of the x-y phase space for a solenoid field of 30 Gauss, 4 RF bucket bunch spacing configuration.

IV. ELECTRON-CLOUD INTENSITY THRESHOLD

A threshold for the electron-cloud was observed [2] between 700 mA to 900 mA with 692 bunches spaced 4-RF buckets at PEP-II. The measurement was carried out without or with the solenoid field of 30 G. To understand the threshold mechanism, we run simulations with the similar parameters as in the experiments. The results of the simulation are shown in Fig 6. It is clearly seen from the figure that there exists a threshold beyond which the density of the electron cloud grows until it reaches equilibrium. The threshold is independent of the bunch spacing S_b if one retains $S_b B_s$ as a constant. Above threshold, the saturated density is proportional to the line density of the beam N_p/S_b indicating it is limited by the space charge. Since the peak beam current at PEP-II is already operated well above the threshold, the simulation predicts that a two-fold increase of the electrons when the bunch spacing is shorten from $4S_{FR}$ to

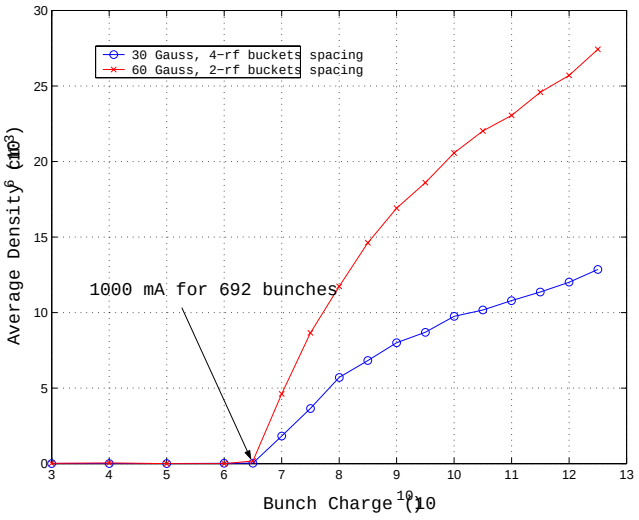

FIG. 6: Saturated density as a function of the bunch population. The circles represent the case of 4-RF spacing and 30 G solenoid field. The crosses represent 2-RF spacing and 60 G field.

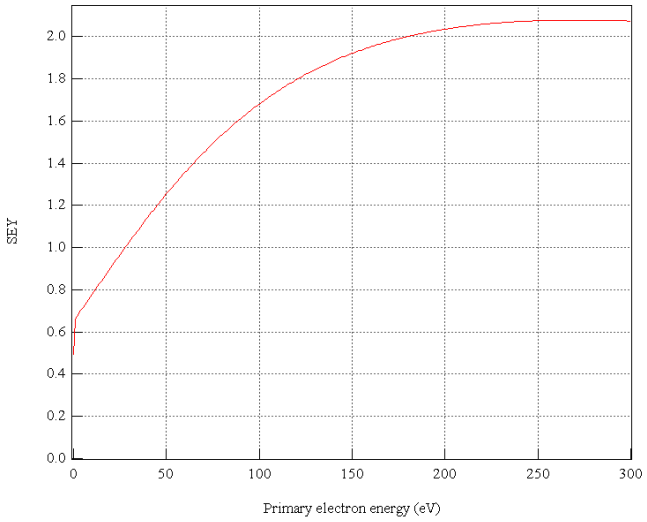

FIG. 7: Details of the secondary electron yield model used for the simulations. The secondary yield exceed 1 for a primary electron energy of 25 eV. Note that the value of the secondary electron yield close to a primary energy 0 eV incident electron energy is $\delta(0) \sim 0.6$.

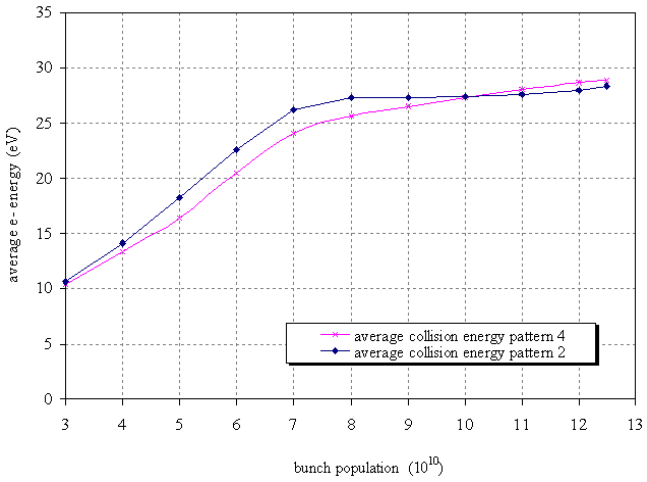

FIG. 8: Average collision energy during the whole simulation run for different bunch population. The average energy reaches 25 eV needed to exceed a unitary secondary yield when the bunch population is $\sim 6.5 \times 10^{10}$, explaining the intensity threshold shown in Fig. 6.

$2S_{RF}$ even if the solenoid field is doubled.

The threshold in the simulation is about 6.5×10^{10} compared with $(4.6-6.0)\times 10^{10}$ in the observation. One should take into account that the effective peak of the secondary electron yield at the vacuum chamber surface may be smaller than 2 as assumed in the present simulation.

A possible explanation of the intensity threshold is given by considering the details of the secondary electron yield as shown in Fig 7. The SEY exceeds unity in our model for a 25 eV primary electron energy. Then, inspecting Fig 8, which shows that the average collision energy of the electrons reaches 25 eV for a bunch population of $\sim 6.5\times 10^{10}$, one may explain the intensity threshold as observed in Fig. 6.

Without solenoid, however, the simulation disagrees with the observation because the absence of the nearby threshold in the simulation.

For an electron near the wall, the momentum kick due to a bunch is given by [7]

$$\Delta p \simeq -\frac{e^2 N_p}{c}\frac{2}{r_b} \tag{4}$$

and thus the energy received from the bunch is

$$\Delta E \simeq \frac{2mc^2 N_p^2 r_e^2}{r_b^2} \tag{5}$$

where r_e is the classic radius of electron. If the electron reaches the wall before the next bunch arrives ($B_s > B_s^c$), multipacting of electrons occurs if

$$\Delta E \geq E_{\delta=1} \tag{6}$$

where $E_{\delta=1}$ (typically 20-100 eV) is the energy above which the secondary yield δ exceeds unity. This yields the threshold of bunch population

$$N_p^{th} \simeq \frac{r_b}{r_e}\sqrt{\frac{E_{\delta=1}}{2E_0}} \tag{7}$$

where $E_0 = mc^2$. In this simulation, we have $E_{\delta=1} \simeq 30$ eV. Using Eq. (7), we obtain $N_p^{th} \simeq 8.8 \times 10^{10}$ compared with 6.5×10^{10} found in the simulation. Besides reducing the secondary yield, enlarging the radius of beam pipe may be more effective way to increase the threshold as indicated in Eq. (7).

We compute the average electron density in the vacuum beam pipe compared with the electron density within an ellipse centered on the beam axis, with and without solenoid field as shown in Fig 9. The area of the beam-ellipse is 20 σ_x x 20 σ_y = 14 mm x 4.6 mm. In particular, for a for a bunch spacing of $S_B = 3\,S_{RF}$, the electron density near the beam reaches $7 \times 10^4 e/cm^3$ when the solenoid field is set at 30 Gauss.

V. MULTI-BUNCH INSTABILITY

A. Calculation of the Vertical Dipole Wake Field Induced by the Electron-cloud

For the calculation of the wake function we follow [12] as reported in [7]. After the electron-cloud have reached an equilibrium density a single perturbing bunch is displaced from the central orbit by an amount Δy. In these simulations, we displace the 40th bunch vertically by Δy=5 mm. The electron cloud is perturbed dynamically causing a dipole wake which affects the subsequent bunches. Let the Δp_y be the momentum kick experienced by the subsequent bunches as they traverse a section of length L. Assuming that there are N sections in the ring, the dipole wake field is computed as

$$W_y(z) = -\frac{NL\overline{F}_y}{qQ\Delta y} = -\frac{cN}{(eN_p)^2}\frac{\Delta p_y}{\Delta y} \tag{8}$$

where $\overline{F}_y = \Delta p_y/\Delta t$ is the force acting on the subsequent bunch during the traversal of the section, Δp_y is the actual momentum kick computed in the simulation and $\Delta t = L/c$. By extracting the dipole wake function we compute the multi-bunch oscillation frequency in the first order approximation given in [12]. Considering the ring filled with M equally-spaced bunches, we compute the coherent dipole frequency Ω_μ corresponding to the dipole oscillation mode μ by

$$\Omega_\mu - \omega_\beta = \frac{ce^2 N_p}{4\pi E\nu_\beta}\sum_{k=0}^{nw} W(ks_B)e^{2\pi ik(\mu+\nu_\beta)/M} \tag{9}$$

where $\omega_\beta = \omega_0\nu_\beta$ is the betatron angular frequency, ν_β is the horizontal or vertical tune, the collective mode oscillation number is given by $\mu = 0, 1, 2...M-1$, E is the beam energy, and the overall summation is extended to the wake computed for the first subsequent bunches, here nw=10. Since the amplitude of the oscillation for each mode μ is proportional to $exp(-i\Omega_\mu t)$, the mode is unstable when ImΩ_μ is negative and damped when positive. Simulation results show that the wake is short range and is significant for few trailing bunches following the perturbing bunch. Thus with good approximation, the instability growth rate τ_0^{-1} is given by the first k=1 term as

$$\tau_0^{-1} = \frac{ce^2 N_p}{4\pi E\nu_\beta}|W(s_B)| \tag{10}$$

the growth rate as a function of the solenoid field are shown in Fig. 11 and in Table II. we make here the approximation of a constant electron density along the circumference C of the ring. Finally noting that the k=0 mode is real and independent of the mode number μ, it is interpreted as the overall coherent tune shift with the analytical expression given by

$$\Delta\nu_\beta = \frac{e^2 CN_p}{8\pi^2 E\nu_\beta}|W(0)|. \tag{11}$$

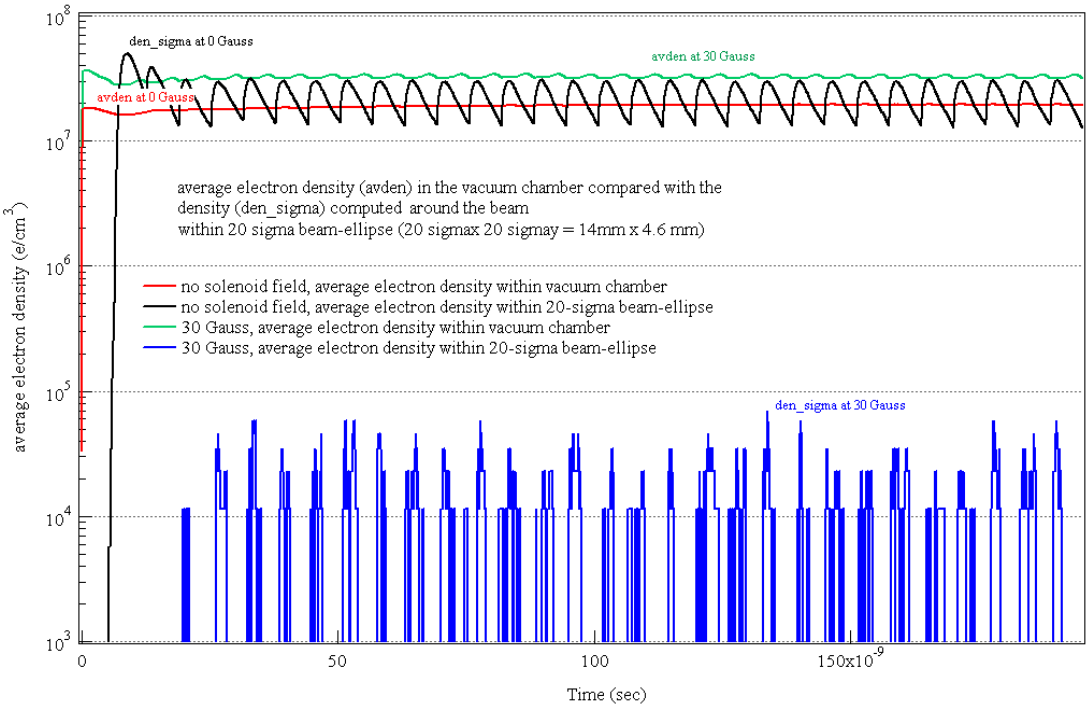

FIG. 9: Average electron density in the vacuum beam pipe compared with the electron density within an ellipse centered on the beam axis, with and without solenoid field. The area of the beam-ellipse is 20 σ_x x 20 σ_y = 14mm x 4.6 mm. The electron density near the beam reaches 7 $\times 10^4 e/cm^3$ when the solenoid field is set at 30 Gauss.

B. Effect of the Solenoid Field on the Wake Field

As the solenoid field increases, the electrons are gradually confined within the vicinity of the wall. However, under the condition of a cyclotron resonance, there exist even more electrons than without solenoid. Since the electrons are confined far away from the beam axis, it is not clear if these electrons could cause any instability.

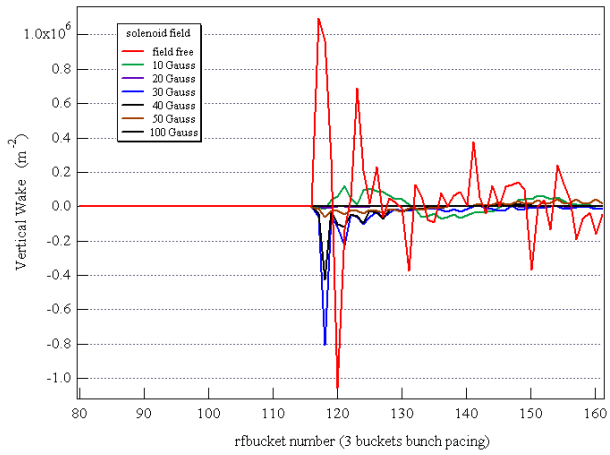

FIG. 10: Long-range wake function due to electron cloud for a bunch spacing $S_b = 3\,S_{RF}$.

To answer this question, we compute the long-range wake as a function of the solenoid field and estimate the growth rate $1/\tau$. The wakes are shown in Fig 10. For these following simulations, we have assumed a bunch spacing $S_b = 3S_{RF}$. Clearly from Fig 10, the peak values of the wake are comparable at $B_s = 0$ and $B_s = 30$ G (at the resonance). The growth time are $\tau = 31, 9870, 145\mu s$ at $B_s = 0, 20, 30$ G respectively. The growth rates and the vertical tune shifts as a function of the solenoid field are shown in Fig. 11 and Fig. 12 respectively. Growth rates and the tune shifts are also shown in Table II.

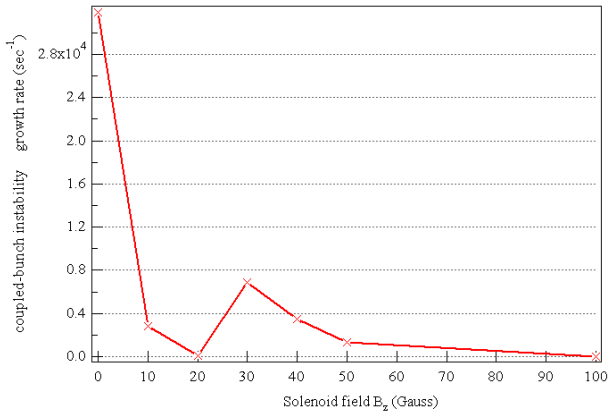

FIG. 11: Multi-bunch instability growth rate as a function of the the solenoid field. The multipacting resonance condition at 30 Gauss is shown in figure for a bunch spacing $S_b = 3\,S_{RF}$.

As the solenoid field increases, one may notice that the computed long-range wake function and the vertical tune shift are changing sign, from positive to negative.

Without solenoid field the tune shift generated by the electrons is positive because the electron-cloud has a focusing effect on the positron beam. As the solenoid field increases the electrons are confined near the wall resulting in a change of sign of the tune shift similarly to a conventional impedance. A neutral behavior at 20 Gauss is expected in the by 3RF bucket spacing.

TABLE II: Multi-bunch instability (MBI) simulations. Electron cloud induced vertical tune shift $\Delta\nu_\beta$ and instability growth time as a function of the solenoid field for a bunch spacing $S_b = 3S_{RF}$.

Gauss	$\Delta\nu_\beta$	τ_0 (μsec)	τ_0^{-1} (1/sec)
no field	0.037	31	31900
10	0.004	357	2800
20	-0.000392	9.8×10^3	101
30	-0.028389	145	6885
40	-0.0369218	288	3467
50	-0.00227659	754	1325
100	1e-06	2×10^6	0.5

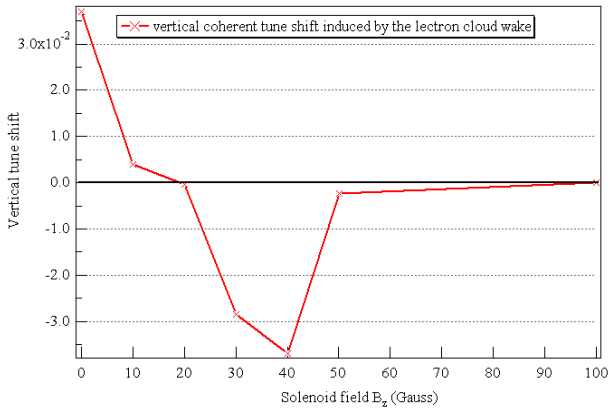

FIG. 12: Vertical tune shift induced by the electron-cloud for a bunch spacing $S_b = 3\,S_{RF}$.

VI. DISCUSSION

Based on the simulation, we find that the cyclotron motion of electrons plays important role in generating and accumulating secondary electrons. When the resonance condition is satisfied, we see huge amount electrons near the wall. Although they are far away from the positron beam, they still create the long-range wake strong enough to cause multi-bunch instability.

In addition, if the solenoid field is strong enough $B_s > B_s^c$, we find that there exists a threshold for the electron-cloud under which there is no accumulated electrons. This discovery may provide us a method to completely eliminate the electron cloud with larger enough beam pipe and lower enough secondary yield.

VII. ACKNOWLEDGMENTS

We would like to thank Franz-Josef Decker, Stan Ecklund, Artem Kulikov, Sam Heifets, John Seeman, Mike Sullivan, and Uli Wienands for many helpful discussions. We are grateful to NERSC for supercomputer support.

[1] H. Fukuma *et al*, in the *Proceedings of the Accelerator Conference* EPAC 2000, Vienna, Austria, 2000, p. 1124.
[2] A. Kulikov *et al*, in the *Proceedings of the Accelerator Conference* PAC01, Chicago, IL, US, 2001, p. 1903.
[3] F. Zimmermann, CERN SL-Note-2000-004 AP(2000).
[4] M.A. Furman and M. Pivi Phys.Rev. ST AB **5**, 124404, 2002.
[5] R. Kirby, SLAC 2003, private communication.
[6] V. Baglin, I. Collins, B. Henrist, N. Hilleret, G. Vorlaufer CERN LHC Project Report 472, 2001.
[7] M. A. Furman and G. R. Lambertson LBNL Note LBNL41123/CBP Note246, SLAC Note PEP-II AP Note AP 97.27.
[8] M. A. Furman Am. J. Phys. **62**(12), Dec. 1994, pg. 1134-1140.
[9] Y. Cai, in the *Proceedings of the* ECLOUD-02 workshop, CERN, Geneva, Switzerland, 2002, p. 141.
[10] O. Gröbner, in the *Proceedings of the* Particle Accelerator Conference (PAC 97), Vancouver, Canada, 1997, and as CERN LHC-Project-Report-127(1997).
[11] A. Novokhatski and J. Seeman in the *Proceedings of the Accelerator Conference* PAC03, Portland, Oregon, US, May 2003.
[12] A.Chao *Physics of Collective Beam Instabilities in High-Energy Accelerators* (John Wiley & Sons, Inc. 1993).